Chapter

Thermoelectric Control of Deep UV LED to Improve Optical Performance

Pablo Fredes, Ulrich Raff, Ernesto Gramsch, Javiera Cuenca and Jose Pascal

Abstract

A thermoelectric control system using thermoelectric cooler devices (TEC) combined with an aluminum heat dissipater and a fan heat extractor allows improving considerably the optical performance of deep UV LEDs (285 nm) operating at desired temperatures. A proportional, integral, and differential controller (PID) control technique was implemented to control the voltage in the TEC devices, and therefore, the desired range of temperatures can be achieved. The PID parameters are obtained with computational simulations based on physical models and experimental data recordings of the temperature, using a thermistor sensor for the temperature measurements and SiC photodiode with UV enhanced system for the optical power measurements. The experimental data show that decreasing the temperature of the UV-C LED light source using a TEC increases the optical output power, while it has been shown that the lifetime of the LED devices can be improved.

Keywords: thermoelectric cooler, optoelectronics, ultraviolet, light-emitting diode, temperature

1. Introduction

Manufactures of new solid state light sources have focused the attention to deep UV light sources (200–300 nm), where UV-C LEDs (or deep UV-LEDs) have shown great potential in many technological applications, such as water and surface disinfection processes, biomedical instrumentation systems, high density optical recording, lithographic micro fabrication, and biophotochemical research [1–4]. The complexity of a reliable UV-C LED performance depends upon optical efficiency, adequate lifetime, and wavelength accuracy that all concern technological applications. It is known that the UV-C LEDs have lower external quantum efficiency (EQE) with a value less than 10%, compared with conventional LED light sources, for example, blue LED (400–450 nm) has an EQE > 70%. In microbiological research, the shift of the peak wavelengths would result in an inaccurate interpretation in microbial studies [5].

2. Efficiency droop and optical performance of UV-LEDs

The optical performance of the UV-LED devices has been studied by Kheyrandish et al. showing that higher solder point temperatures (T_S) resulted in lower optical output power, shift of the peak wavelength, and an increase of the full width at half maximum (FWHM) [5]. The achieved internal quantum efficiency (IQE) of UV-C LEDs can be quite high, that is, somewhere between 15 and 70%, supported by photoluminescence studies and ray-tracing calculations. However, the external quantum efficiency and the radiant efficiency of UV-C LEDs are below 2% (highest for 280 nm LEDs) [6]. Nevertheless due to increasing development efforts, the UV-C LED devices have much lower output power from single chip than the widely used blue LEDs.

The optical performance of a UV-C LED device decreases, due to a variety of key factors such as quantum-confined Stark effect, carrier delocalization, and others discussed by Versellesi et al. [7]. It is possible to make a classification of droop mechanisms in two levels. The first classification level reflects nonradiative losses taking place inside the optical active region and the second level reflects nonradiative losses taking place outside the optical active region.

Until recently, the principal cause of efficiency droop was unclear in AlGaN LEDs (from blue to UV-C sources). The Auger effect has been proposed as the main cause of efficiency droop in InGaN LEDs. Thanks to Iveland's contribution with direct measurement of Auger electrons emitted from LEDs under electrical injection of high currents, it was possible to conclude that the efficiency droop phenomenon finalized a long-standing controversy [8].

2.1 Thermal stress and lifetime performance

The excessive self-heating of the UV-C LED reduces the lifetime of the devices, the optical performance, and yield spectral shift of the emission. Lifetime limiting issues of UV-C LED occur with high thermal stress in the chip, resulting from the higher electrical current (100–350 mA). The device lifetime may be difficult to assess, in a rigorous fashion. Nevertheless, one recent published result has shown that the lifetime decreases more with a current of 350 mA than with 100 mA in UV-C LEDs by Nikkiso Co, LTD [9]. The thermal extraction is one of the challenges to improve the performance of the LED devices [10]. To resolve this challenge, the thermal conductivity of the package must be considered. The relation between thermal conductivity and thermal resistance is known, and therefore, thermal resistance provided by the manufacturer will be considered.

2.2 LED package and junction temperature

Various indirect techniques and models have been reported for junction temperature T_J measurement techniques including micro Raman spectroscopy, threshold voltage, thermal resistance, photo thermal reflectance microscopy (PRM), electroluminescence, and photoluminescence [11]. In this work, the junction temperature T_J has been obtained applying a thermal resistance technique and direct measurements of the solder point temperatures T_S [12]. The UV-C LED manufacturer allows to compute the optical efficiency of our 285 nm UV-C LED model: VPS171 by Nikkiso Co. The maximal operational solder temperature value can be determined using the maximal junction temperature provided by the manufacturer. The solder point temperature T_S and the junction temperature T_J are linearly related, as shown

in (1), where I_{LED} is the electric LED current and V_{LED} is a forward LED voltage. Wall plug efficiency (WPE) will be defined in the next section.

$$T_J(t) = T_S(t) + R_{J-S}(1 - WPE)\, I_{LED}\, V_{LED} \tag{1}$$

3. Wall plug efficiency and temperature dynamics

The wall plug efficiency (WPE) is defined as the ratio of electrical power consumption P_{LED} and optical output power of the UV-C LED device denoted by P_{LIGHT}. Kneissl related the WPE with external quantum efficiency (EQE) and the rate between optical and electrical energy [13] as shown in the next equation.

$$WPE = \frac{P_{LIGHT}}{P_{LED}} = \eta_{EQE}\frac{h\nu}{eV} \tag{2}$$

where h is the Planck's constant, ν is the frequency of the UV light, e is the elementary electric charge, V is the voltage, and η_{EQE} is the external quantum efficiency factor.

The ratio of the number of photons emitted from the LED per second to the number of carriers (electrons) injected into the device per second is precisely EQE. The data sheet of our 285 nm UV C LED showed that at 350 mA and 6 V, the UV-C LED can provide an optical output power of 30 mW. This implies that the WPE is 1.43% and EQE is 1.97%, that is, that 1.97% of the injected electrons is converted to UV-C light. Eq. (2) shows that the optical output power P_{LIGHT} is related with P_{LED} and the temperature, and its relation with EQE is shown in Eq. (3)

$$P_{LIGHT}(T_J) = \eta_{EQE}(T_J)\frac{h\nu I_{LED}}{e} \tag{3}$$

Eq. (3) allows to relate the EQE with the junction temperature. Since the junction temperature can be controlled, the EQE factor (η_{EQE}) can be improved.

Joule's first law shows the relation between the heat generated by an electric current passing through a conductor. Eq. (4) shows that the electrical power is converted to light and heat.

$$P_{LED} = I_{LED}\, V_{LED} = P_{LIGHT} + P_{HEAT} \tag{4}$$

The light power P_{LIHT} can be determined using the electrical efficiency factor WPE, obtained with the parameters of the UV-C LED provided by the manufacturer as a linear relation, $P_{LIGHT} = WPE\ P_{LED}$.

As shown in **Figure 1**, P_{HEAT} is divided into two heat transfer rates. *P1* is the heat transfer rate between the junction surface and the ambient environment, and *P2* is the heat transfer rate between the junction surface and the cooling system. For operations at ambient temperature, P_1 is negligible compared to P_2.

3.1 Newton's law of cooling

The thermal performance of the UV-LED device shows that the solder temperature dynamics $T_S\ (t)$ can be modeled with Newton's law of cooling, where T_{EST} represents the temperature in the steady state.

$$\frac{dT_S}{dt} = -K(T_S - T_{EST}) \tag{5}$$

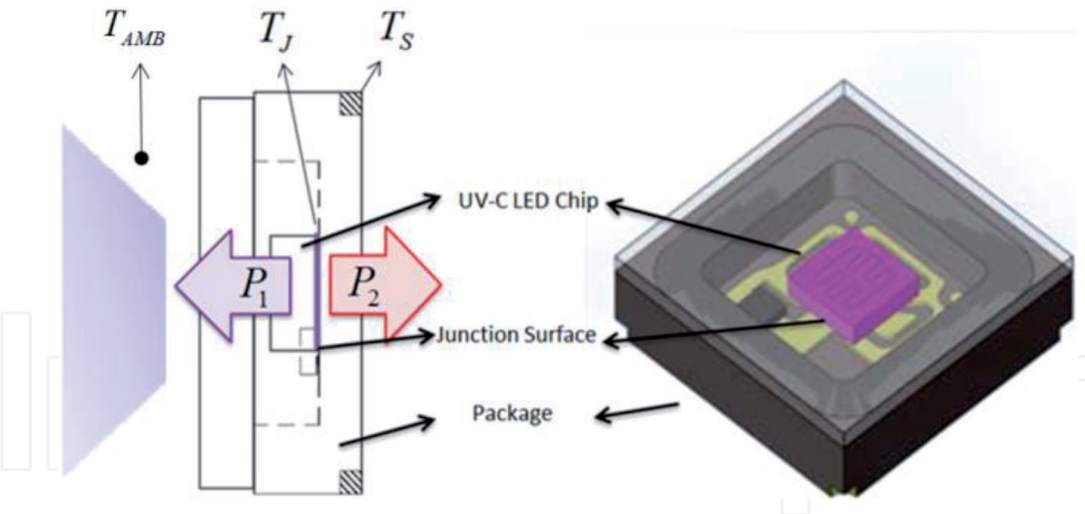

Figure 1.
UV-C LED chip inside the package represented in 2D and 3D diagrams. The size of the LED package shown at the right-hand side is 3.6 × 3.6 mm. T_{AMB} is the ambient temperature, T_J is the junction temperature, and T_S is a solder point temperature.

Taking into account that the cooling process begins at ambient temperature T_{AMB}, commonly in the range of 19–25°C, to finally achieve the steady state of the temperature T_{EST}. The analytical solution for the solder temperature is

$$T_S(t) = T_{EST} + (T_{AMB} - T_{EST})\, e^{-Kt} \tag{6}$$

Commonly, the inverse of the constant K is referred to as time constant of the system. The determination of the constant K of Newton's law of cooling is important and has to be determined experimentally for each LED device (including thermoelectric cooler system). The K value depends on the predefined stationary temperature value T_{EST}. The value of the cooling temperature constant K will be able to model the thermal performance of the system. Therefore, the UV-C LED device temperature can be controlled applying a corresponding strategy.

4. Experimental setup

Our setup is composed by three essential parts: the UV-C LED device, the optical sensor (SiC photodiode model: SG01D-C18, from SGLux), and the temperature sensor (calibrated thermistor). The UV-C LED system is mounted on an optical table (**Figure 2B**). The light output is directed toward an optical sensor at a predefined distance, and finally, a temperature sensor is mounted at the solder point. Experimental data are acquired using a computational interface.

The thermoelectric cooler cell (TEC) is composed of a large number of PN and NP semiconductor arrays. TEC modules can convert voltages (V_{TEC}) into a temperature gradient, based on a phenomena discovered by Peltier in 1834. In this study, a TEC model number TEC1-12706 by Hebei I.T. Co. Ltd. was used.

The experimental setup for the measurements of solder temperature dynamics T_S consists of a 10 kΩ thermistor model NTC Murata, which is directly put in contact on the solder point. The temperatures are measured at the edge of the LED package shown in the right-hand side of **Figure 1**. The thermistor is powered by a stabilized voltage source device, model: LM2596 DC-DC. The signal of the thermistor is connected to an A/D converter to acquire and record (every second) the temperature data.

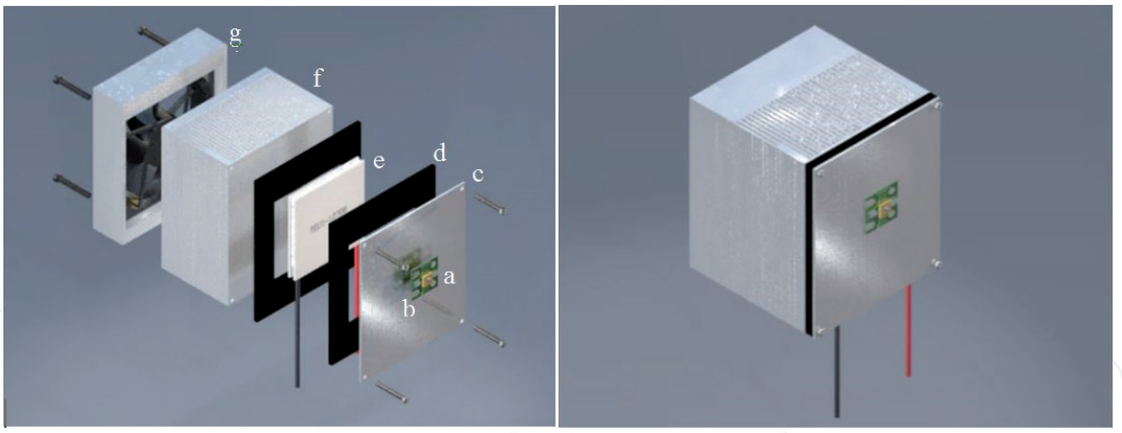

Figure 2.
Components of the UV-C LED device (A): (a) UV-C LED SMD chip, (b) MCPCB, (c) aluminum plate, (d) thermal isolators, (e) thermoelectric cooler device (TEC), (f) aluminum heat dissipater, and (g) fan heat extractor. (B) All components shown in (A) are mounted.

The accuracuty of our thermistor is 1%, specified by the manufacturer, our operation range is from −40 to 60°C, therefore the maximum absolute error is ε1 = 1°C. The computational interface error is ε2 = 0.5°C. It is possible to estimate the standard error of the mean (SEM) for the temperature measurements, using the standard deviation of 20 repetitions of the data recorded for a fixed value of temperature, monitored by a thermal camera model FLIR E 63900 with an emissivity setting of 0.95. The standard deviation was S = 0.73°C, and the total error for the temperature recording can be estimated, that is, ε3 = 0.16°C. Finally, to complete the total error of the solder point temperature measurements T_S, we sum all previously mentioned errors Δ = ε1 + ε2 + ε3 = 1.66°C. Previous work shows that the standard deviation between the modeled and true junction temperatures for blue LEDs was only 3.5°K [14].

5. Thermal performance and empirical modeling

5.1 Thermal resistance

The thermal partial resistances correspond to the various functional groups in the system or heat path and characterize their individual thermal behavior (**Figure 3**). The total thermal resistance *R* of the system is then equal to the sum of the individual thermal resistance components.

$$R = R_{J\text{-}S} + R_{S\text{-}B} + R_{B\text{-}TEC} + R_{TEC\text{-}AL} + R_{AL\text{-}AMB} \tag{7}$$

$R_{J\text{-}S}$ is the thermal resistance of the UV-C LED chip and describes the transfer of heat within the LED housing (junction-to-solder-point), $R_{S\text{-}B}$ is the thermal resistance of the solder point to the metal core printed circuit board (MCPCB), $R_{B\text{-}TEC}$ is the thermal resistance of the MCPC and aluminum plate to the thermoelectric cooler device (TEC), $R_{TEC\text{-}Al}$ is the thermal resistance of the TEC to the aluminum heat dissipater, and finally $R_{AL\text{-}AMB}$ is the thermal resistance of the aluminum heat dissipater to the ambient environment. The thermal resistance between board and TEC ($R_{B\text{-}TEC}$) is not strictly a thermal resistance, but it is technically a heat engine, which can be considered a peculiar thermal resistance with negative value [15]. It is clear that this is an advantage of the TEC, since it can be observed in (7), that

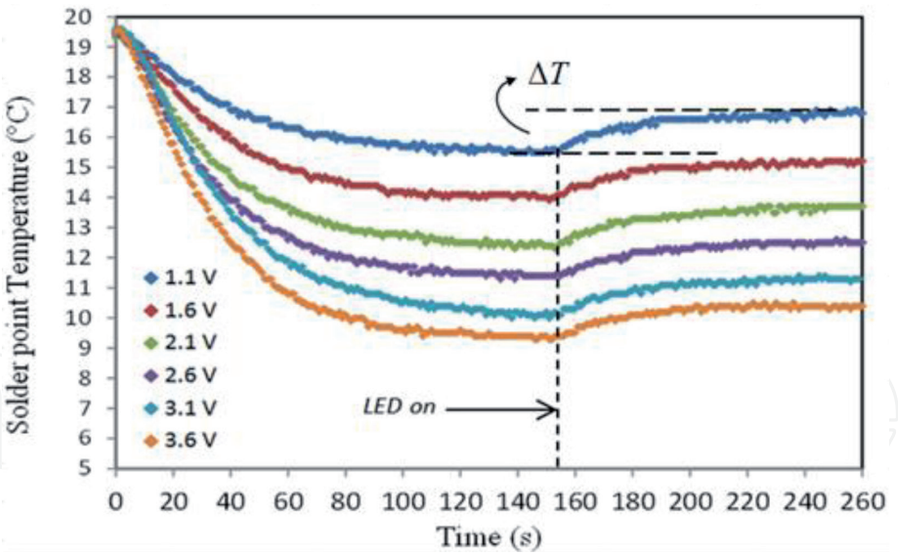

Figure 3.
Performance of solder temperature as a function of time for different values of TEC voltages. The dotted vertical line shows the time when the UV-C LED is turned on after the first stationary temperature obtained from the TEC. The difference between first and final stationary temperatures is given by ΔT.

the negative value of $R_{B\text{-}TEC}$ reduces the total thermal resistance of the device. As a general rule, the smaller the thermal resistance of a LED, the faster the heat can be dissipated from the housing.

5.2 Thermal performance

To obtain the stationary temperature of the system T_{EST} and its relationship with TEC voltage, we apply a pre-cooling turning on of the LED. First, the TEC is turned on with a predefined constant voltage value. Once the stationary temperature is reached, the UV-C LED source is turned on. The system will then reach its final stationary temperature.

T_{EST} is related with V_{LED} and T_{AMB}. It is possible to achieve the stationary temperatures in the system making the cooling process with the TEC before turning on the LED. It is known that the relation between TEC voltage and gradient temperature is linear. The linear relation is described in the following equation.

$$T_{EST}(V_{TEC}, T_{AMB}) = T_{AMB} - mV_{TEC} \quad (8)$$

If T_{AMB} is constant, it is possible to obtain the value of slope m, relating the empirical recording of the cooler process dynamics, for different values of V_{TEC}. The value of m is a thermal property of each system, in a specific range of temperatures. For example, the data displayed in **Figure 3**, allow to confirm the linear relationship stipulated in Eq. (8), that is, $T_{EST} = 19.5–1.59V_{TEC}$. In the six curves shown in **Figure 3**, V_{LED} was maintained constant.

6. Temperature control using TEC and PID controller

The control technique implemented in this application has been developed applying the previously described physical model, the results of the simulations, and the recorded experimental temperature data.

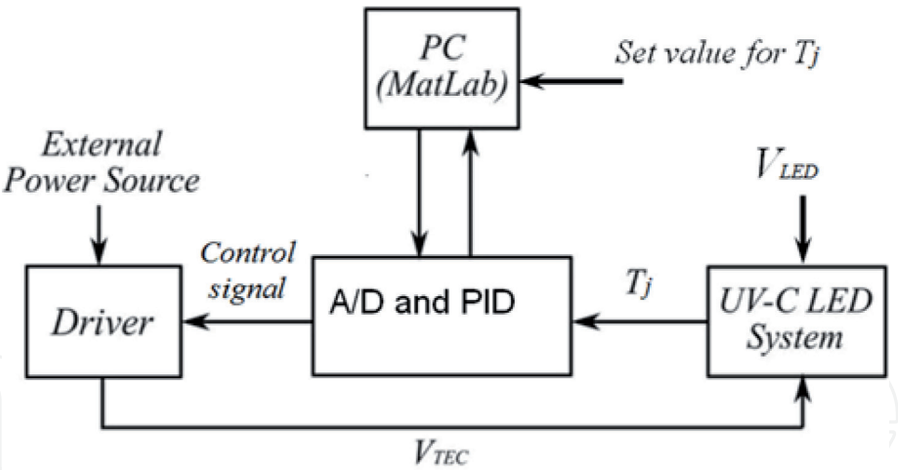

Figure 4.
Schematic diagram for the temperature controller.

According to Eq. (1), the solder point temperature can be obtained knowing the junction temperature. We can define a reference junction temperature $T_{J\text{-}REF}$ and obtain a stationary reference solder point temperature $T_{EST\text{-}REF}$. The controller operates comparing $T_{EST\text{-}REF}$ to $T_S\ (t)$ to obtain an error signal that is fed to the PID controller. The PID controller applies V_{TEC} to the system to yield $T_{EST\text{-}REF}$.

The block diagram displayed in **Figure 4** is implemented with the MATLAB Simulink software, considering the empirical values of the time constant, the ambient temperature T_{AMB}, the increment ΔT, the linear relation between V_{TEC} and T_{EST} shown in Eq. (8), and the set values for the junction temperatures $T_{J\text{-}REF}$.

7. Results

A computational tuning based on a simulated plant is used to obtain the PID parameters, which were then applied and verified experimentally. For each steady-state temperature T_{EST}, the PID parameters can be obtained in the simulations to be consequently applied in the controller (**Figure 5**).

Using these gain parameters for the PID controller applied to our system, we can fit the simulations of the temperature dynamics for three different steady-state operations. When the UV-C LED is turned on, the control of the system increases the TEC voltages to recover the starting temperature states as displayed in **Figure 6**.

One of the major advantages of the temperature control is the improvement of the optical output power. This result is displayed in **Figure 7**. The relation between junction temperature and UV intensity shows that as the temperature drops, the UV intensity increases. The plotted data demonstrate that reduction of the junction temperature T_J from 59 to 44°C increases the UV irradiation by 6%.

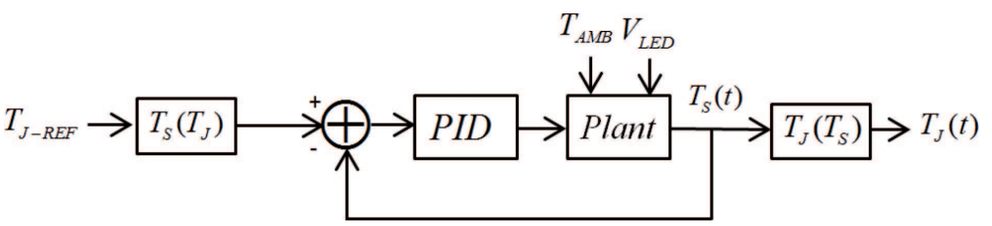

Figure 5.
Block diagram for PID controller of T_J based on T_S control.

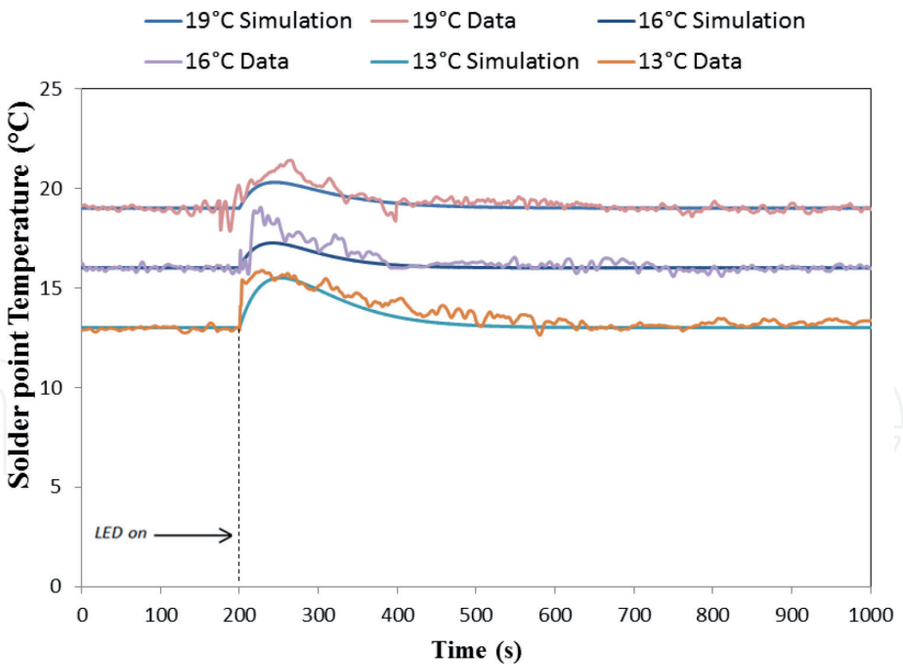

Figure 6.
Fit of the simulations and experimental temperature dynamics for three different steady-state operations after initial precooling.

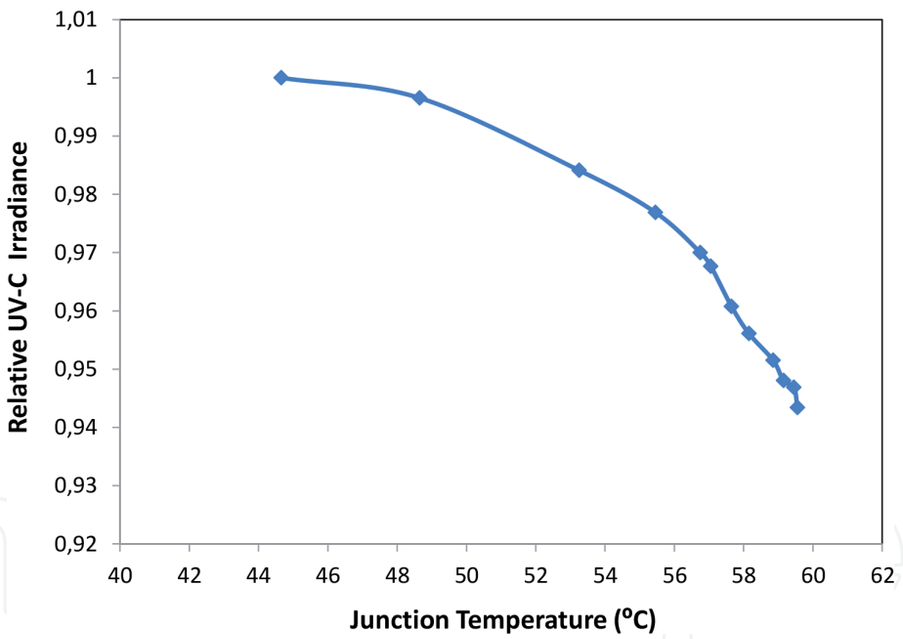

Figure 7.
Normalized irradiance as a function of junction temperature.

8. Conclusions

The result shows that the TEC can effectively reduce the thermal resistance of the high power UV-C LED device and therefore substantially increase the optical performance. In addition, the lifetime might be highly improved [8]. Since the system temperature affects the optical performance, it is essential to control it. The TEC device makes it possible to implement an appropriate control strategy. Each LED device has different thermal performance, depending on many factors, for example, thermal conductivity of the heat dissipaters, the fan extractor velocity, and operation ambient temperature. At lower temperature operations, optical

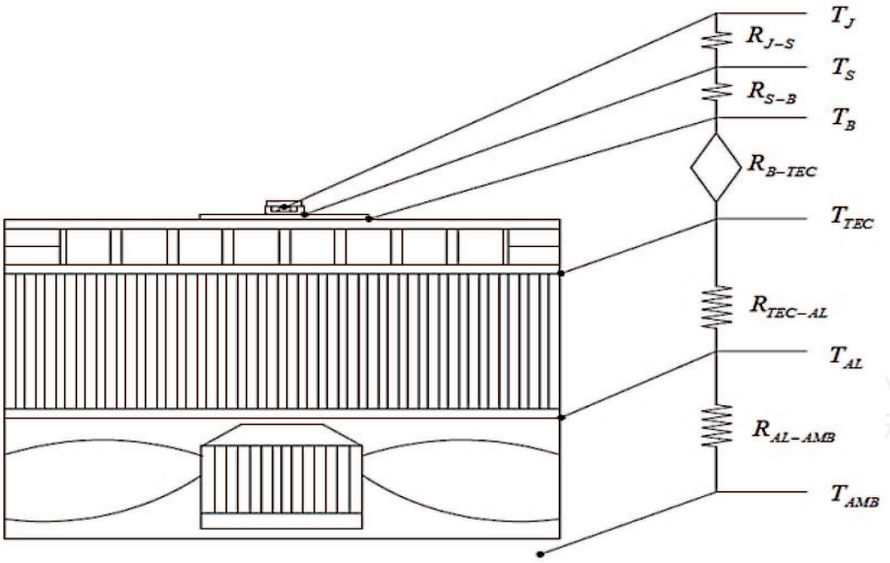

Figure 8.
Representation of a UV-C LED system, describing the series of thermal resistances and the points of the thermal interfaces, specified on the right hand side.

performance is improved. The operation of the UV-C LED at lower temperatures implies that the intrinsic lifetime could be substantially improved. The implementation of the TEC device for the thermal control of the UV-C LED light source allows an efficient optimization of the optical performance (**Figure 8**).

Acknowledgements

Portions of this work were presented at the OSA Light, Energy and Environment Congress in November 2017, titled "Improving the Optical Performance and Life Time of Deep UV LEDs by Thermoelectric Control". This work was supported in part by for the Hydraluvx Spa, Santiago, Chile and Mrs. Andrea Bravo, Hydraluvx's Graphics Designer, Santiago Chile is gratefully acknowledged for the rendering of **Figures 2** and **8**.

Author details

Pablo Fredes*, Ulrich Raff, Ernesto Gramsch, Javiera Cuenca and Jose Pascal
Department of Physics, Universidad de Santiago, Chile

*Address all correspondence to: pablo.fredes@usach.cl

References

[1] Khan A, Balakrishnan K, Katona T. Ultraviolet light-emitting diodes based on group three nitrides. Nature Photonics. 2008;**2**:77-84

[2] Sholtes KA, Lowe K, Walters GW, Sobsey MD, Linden KG, Casanova LM. Comparison of ultraviolet light-emitting diodes and low-pressure mercury-arc lamps for disinfection of water. Journal of Enviromental Technology. 2016;**37**:2183-2188

[3] Hirayama H, Maeda N, Fujikawa S, Toyoda S, Kamata N. Recent progress and future prospects of AlGaN-based high-efficiency deep-ultraviolet light-emitting diodes. Japanese Journal of Applied Physics. 2014;**53**:100209

[4] Inoue S, Tamari N, Taniguchi M. 150 mW deep-ultraviolet light-emitting diodes with large-area AlN nanophotonic light-extraction structure emitting at 265 nm. Applied Physics Letters. 2017;**110**:141106

[5] Kheyrandish A, Mohseni M, Taghipour F. Development of a method for the characterization and operation of UV-LED for water treatment. Water Research. 2017;**122**:570-579

[6] Schur MS, Gaska R. Deep-ultraviolet light-emitting diodes. IEEE Transactions on Electron Devices. 2010;**57**:12-25

[7] Verszellesi G, Saguatti D, Meneghini M, Bertazzi F, Goano M, Meneghesso G, et al. Efficiency droop in InGaN/GaN blue light-emitting diodes: Physical mechanisms and remedies. Journal of Applied Physics. 2013;**114**:071101

[8] Pernot C. Improving Deep UV LED Performance. Presented at the LED China Conference, Shanghai, China; 2016. http://www.semi.org.cn/semiconchina/mail/160331/1/02-SEMICONCHINA-DUV-LED-cyrilpernot.pdf

[9] Nikkiso Co. Standard Specifications for UV LED, model VPS131, Vol. 1.2; 2016

[10] Kneissl M et al. Development of UV-C LED Disifection. TECHNEAU; 2010

[11] Akca H, Yasa Y, Ayaz R, Durusu A, Ajder A, Nakir I, Tanrioven M. Thermal management of power LED system. In: Proceedings of ICRERA; Milwaukee, WI, USA; 2014. pp. 760-764

[12] Xi Y, Gessmann T, Shah JM, Kim JK, Schuberta EF. Junction and carrier temperature measurements in deep-ultraviolet light-emitting diodes using three different methods. Applied Physics Letters. 2005;**86**:031907

[13] Kneissl M, Rass J. A brief review of III-nitride UV emitter technologies and their applications. In: III-Nitride Ultraviolet Emitters. 1st ed. Vol. 227, Springer Series in Materials Science. 2016. pp. 1-25

[14] Reed ML, Wraback M, Lunev A, Bilenko Y, Hu X, Sattu A, et al. Device self-heating effects in deep UV LEDs studied by systematic variation in pulsed current injection. Physica Status Solidi. 2008;**5**(6):2053-2055

[15] Riffat SB, Ma X. Thermoelectrics: A review of present and potential applications. Applied Thermal Engineering. 2003;**23**(8):913-935